

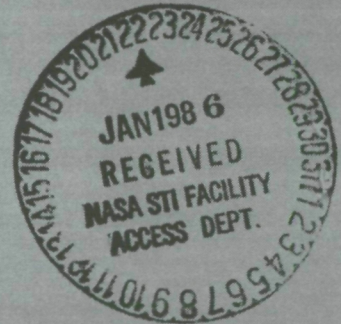
NASA
STAR
(1+3)

C S S A

CONTRIBUTIONS TO
PROCEEDINGS FROM THE NATO ADVANCED RESEARCH
WORKSHOP ON THE SEISMOLOGY OF THE SUN AND
THE DISTANT STARS

CSSA-ASTRO-85-23

September 1985



**CENTER FOR SPACE SCIENCE AND ASTROPHYSICS
STANFORD UNIVERSITY
Stanford, California**

(NASA-CR-176470) CONTRIBUTIONS TO
PROCEEDINGS FROM THE NATO ADVANCED RESEARCH
WORKSHOP ON THE SEISMOLOGY OF THE SUN AND
THE DISTANT STARS (Stanford Univ.) 24 p
HC A02/MF A01 CSCL 03B G3/92 N86-19275
THRU N86-19278
Unclas 03696

CONTRIBUTIONS TO
PROCEEDINGS FROM THE NATO ADVANCED RESEARCH
WORKSHOP ON THE SEISMOLOGY OF THE SUN AND
THE DISTANT STARS

CSSA-ASTRO-85-23

September 1985

The Detection of Global Convective Wave Flows on the Sun by
Philip H. Scherrer, Richard Bogart, and J. Todd Hoeksema of the
Center for Space Science and Astrophysics, Stanford University,
and Hirokazu Yoshimura of the Department of Astronomy, University
of Tokyo.

Observations of Low-Degree P-Mode Oscillations in 1984 by
Harald M. Henning and Philip H. Scherrer

Comments on Techniques for Spectral Deconvolution by
Philip H. Scherrer

This work was supported in part by the Office of Naval Research under
Contract N00014-76-C-0207, by the National Aeronautics and Space
Administration under Grant NGR5-020-559, and by the Atmospheric
Sciences Section of the National Science Foundation under Grant ATM77-
20580.

THE DETECTION OF GLOBAL CONVECTIVE WAVE FLOWS ON THE SUN

Philip H. Scherrer,
Richard Bogart,
J. Todd Hoeksema[†] and,
Hirokazu Yoshimura[‡]

[†]Center for Space Science and Astrophysics, Stanford University

[‡]Department of Astronomy, University of Tokyo

ABSTRACT. Global convective flows in the solar convection zone have been predicted by theoretical interpretations of the global-scale ordering of magnetic fields and activity centers and by theoretical analyses of rotating convection zones. Direct evidence of these flows in the photosphere has not previously been found despite several long-term efforts. The signatures of such flows have now been detected by analyzing the daily series of low-resolution Dopplergrams obtained at the Wilcox Solar Observatory at Stanford University. The signatures are patterns of alternating east and west flows with amplitudes on the order of 25 m/s and longitudinal extent of about 30 degrees. The patterns move across the disc at approximately the solar rotation rate and have lifetimes of at least several rotations. Boundaries of the fast and slow flows are often associated with large magnetic active regions.

The detection and study of global convective wave flows on the sun is of great importance for understanding the basic mechanisms of the generation of magnetic fields and magnetic activity on the sun (Yoshimura, 1971). They have been considered as the most likely kind of fluid motions to drive the solar dynamo which generates magnetic fields on the sun (Yoshimura, 1972, Yoshimura, 1983). This global convection has escaped detection despite a number of long-term observing and analysis programs (Durney et al., 1985, Howard and Yoshimura, 1976, Howard and LaBonte, 1980, LaBonte et al., 1981, Snodgrass and Howard, 1984).

Observations made at the Wilcox Solar Observatory at Stanford University have been examined for the signature of global scale convective motions. This series of observations began in 1976 and has been found to have lower noise in the detection of solar velocities than the instruments used in previous analyses (Scherrer et al., 1980). We now have a sufficient time span of observations to study the evidence for global-scale horizontal motions superimposed on solar rotation. The observations are Doppler-shift measurements which yield low-resolution full-disc daily velocity maps. Clear velocity patterns with amplitudes

of at least 25 m/s have been found in zones near the equator. These patterns can be seen to move across the disc with solar rotation. They have a large latitudinal extent, crossing the equator, but are not aligned on meridians. There are from 4 to 7 alternating patterns around the sun (Scherrer and Yoshimura, 1985, Yoshimura et al., 3-15).

There are several fundamental difficulties in detecting global-scale small-amplitude horizontal motions on the sun. One problem is caused by the large contributions of solar rotation (about 2000 m/s at the equator) and the limb shift (a "W"-shaped red-shift profile across the disc with an amplitude of 600 m/s at the limb and 30 m/s at the disk center). Other sources of solar "noise" are the motions of 5-minute oscillations and supergranulation. These noise velocities are larger in amplitude but smaller in scale than the postulated horizontal flows. The large aperture used for the Stanford observations greatly attenuates these signals. A third solar source of velocity noise comes from the red-shifts associated with regions of intense magnetic fields. These "downflows" have been examined by a number of authors (Cavallini et al., 1985, Labonte and Howard, 1982) and are generally believed to be due to a local reduction in small scale convective motions in the vicinity of magnetic fields.

A final difficulty is that we are restricted to measuring the line-of-sight component of the motion. In order to infer individual velocity components, one must assume either spatial continuity or temporal continuity during the disc passage of individual features. In the present work, we have used two different methods in an attempt to understand and avoid the weaknesses of each. In both approaches, we assume the rotation and limb shift signals are constant over several rotations, and that the remaining horizontal motions are organized on a scale much larger than supergranulation. In the first approach (Scherrer and Yoshimura, 1985) we further restrict ourselves to horizontal velocity structures with a large east-west extent. We assume that by averaging over a large window (up to a solar radius) the components other than east-west motions will cancel. In the second approach (Yoshimura et al., 3-15), we do not assume such a large spatial extent, but we assume that the structures are stable during their disc passage. The two methods have different sensitivities to noise and changing solar velocity fields. We refer to the two methods as the slope method and the decomposition method.

The Stanford velocity maps are a product of a 9-year synoptic series of observations. The observations and instrument have been described previously (Duvall, 1979, Scherrer et al., 1980) and will be only briefly described here. The instrument is a scanning magnetograph attached to a high dispersion spectrograph. The raw data consist of intensity, magnetic field, spectral line position, position on the solar image, and time. Daily scans are made with a three-arc-minute square aperture. The solar image is scanned in 21 steps of 90 arc-sec in the solar east-west direction and stepped to 11 scan lines in the north-south direction. In this way we obtain simultaneous magnetograms and Dopplergrams on every suitable day. The observations are made in the absorption line of neutral iron near 525.02nm. The calibration of the line shift signal in m/s and removal of the earth's motion is done as

described previously. After excluding observations contaminated by clouds we have 1494 daily Dopplergrams for the present study.

Previous analyses have removed the large rotation and limb-shift signal by fitting and subtracting a particular functional form of differential rotation and limb-shift from each Dopplergram. To avoid any spurious signal from an improper fit and to avoid the possibility of removing some of the desired signal as rotation, we have adopted a new procedure. The first step is to subtract the 54-day running mean of the observed velocity at each point on the disc. This procedure removes any signal dependent on disc position, such as rotation and limb shift, without making any assumptions regarding its functional form. Next, we subtract from each scan point residual the mean of all residuals within the central 80% of that Dopplergram. This step is necessary because we have no absolute velocity reference for our measurements. To reduce the contamination of our horizontal velocity signal by active-region redshifts, we next discard all scan points which have a velocity residual amplitude exceeding 30 m/s or a magnetic field exceeding 20 gauss. An average of 27 percent of the scan points were discarded from each Dopplergram. Discarding these points may remove evidence of the larger amplitude flows, but we believe it is necessary to remove most of the contamination from the active regions.

The resulting series of residual Dopplergrams is then analyzed for horizontal velocity components by fitting the east-west component of motion. In the first approach (slope method) we fit the east-west component in a restricted portion of the solar disc with a large longitudinal window at a fixed latitude. This is done by finding (by least squares) the east-west component of velocity (V_{west}) such that: $V_{obs} = V_{west} \sin(L) \cos(B_0)$ where L is the longitude measured from disc center and B_0 is the latitude of disc center. The regions included in each fit were east-west strips 810 arc-seconds long by 180 arc-seconds wide. These fits were computed for the nine central scan lines and all possible east-west positions for each Dopplergram. From these fits we can display daily maps of east-west motions. The relatively large area used in these fits greatly attenuates the noise from oscillations and supergranulation. It also acts as a spatial filter allowing only very large-scale structures to produce a signal. The method is not sensitive to day-to-day variability in instrumental zero or noise from changing solar velocities, but it is sensitive to contamination from line shifts not associated with east-west motion.

We also derived east-west motions by a second approach (decomposition method) in which we examine the Doppler-shift variation of each location on the sun as it crosses the disc. This is accomplished by using all Dopplergrams having a given Carrington coordinate within $0.8 R_0$ of disc center to find the inferred components U , V , and W that best fit (least squares) the observed velocity residual V_{obs} :

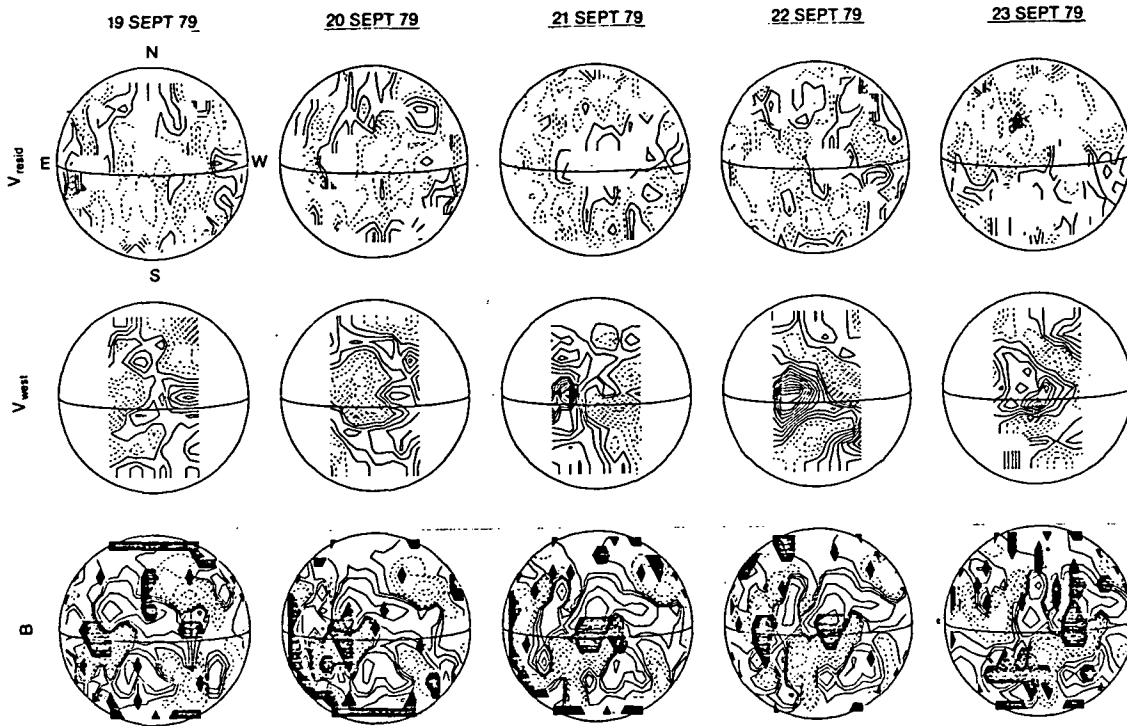


Figure 1: Velocity residual maps for September 19 to 23, 1979. The top row is the line-of-sight "velocity" with limb-shift and rotation removed (positive away from observer). The middle row is the computed east-west velocity (positive to the west) and the bottom row is the magnetic field. The contour levels are 10 m/s for the velocity maps and 0, ± 1 , 2, 5, 10 ... gauss for the magnetograms. The regions excluded from the analysis are shaded on the magnetograms.

$$V_{\text{obs}} = U \cos(B_0) \sin(L)$$

$$+V(\cos(B_0) \sin(B) \cos(L) - \sin(B_0) \sin(B))$$

$$-W(\cos(B_0) \cos(B) \cos(L) + \sin(B_0) \cos(B))$$

where B is the latitude and U , V , W are the westward, northward, and upward components respectively. This method has the advantage that it cleanly separates the westward velocity from active-region "downrafts"

but has the disadvantage that it assumes a static velocity structure, no day-to-day zero level errors, and the Carrington rotation rate.

Using the slope method, Scherrer and Yoshimura (1985) have shown that there are global-scale velocity features that are stable for their transit across the disk. This is the first requirement for detecting large scale flows. Figure 1 shows data from 5 consecutive days, September 19 to 23, 1981. The top row shows residual line-of-sight signals (before excluding points with large residuals or fields), the center row shows V_{west} as described above, and the bottom row shows the corresponding magnetograms for comparison. The V_{west} signal can easily be seen to move across the disc as the sun rotates. The V_{west} signal is shown as positive values with solid contours in regions of westward motion (i.e. motion in the same direction as rotation).

To study the morphology of the horizontal flows we have constructed synoptic charts of both V_{west} and U in the same way as is usually done for magnetic fields. These charts show a map of the solar surface made by averaging the signals from each day's observations for each latitude-longitude bin. The synoptic charts are computed on a grid of 5-degrees in longitude by 30 equal steps in sine-latitude. Some additional temporal and spatial averaging results from this process. To reduce the small-scale noise a further averaging with a 40-degree-in-longitude low-pass filter was applied to each latitude strip.

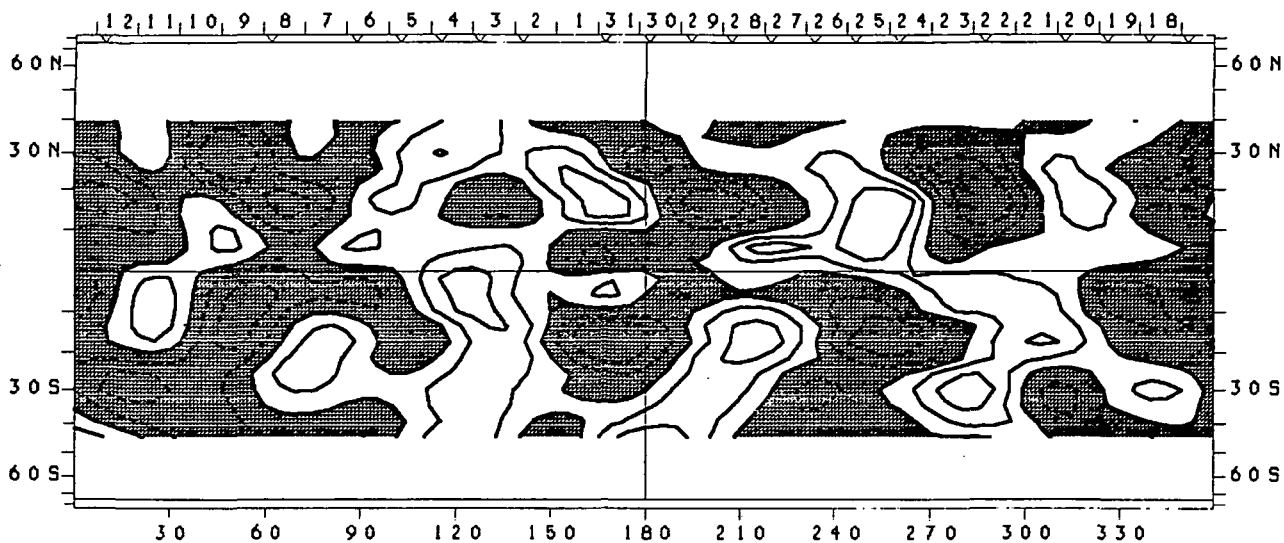
Figure 2a shows V_{west} for three consecutive rotations from the fall of 1979, Figure 2b shows three rotations from the fall of 1981, and Figure 2c shows the fall of 1984. The velocity pattern shows 4 or 5 structures of alternating eastward and westward motion per rotation. These structures are most clearly seen in low northern latitudes. They can be followed for several rotations.

Synoptic maps computed with the decomposition method have roughly the same character but differ in detail. They differ most in the vicinity of active regions, where the slope method could be contaminated by "downflows" if their spatial extent is large, and the decomposition method would be contaminated if they are changing.

This signal appears to persist for more than one rotation. Flows of about the same magnitude are generally present during the past six years during periods of both intense and low magnetic activity. For instance, the signal is present in the fall of 1984 when activity was quite low indicating that the while there is a correlation with the magnetic structures, we really are measuring different physical quantities. A full understanding of the relation between the flow patterns and magnetic activity will require more analysis and more complete observations

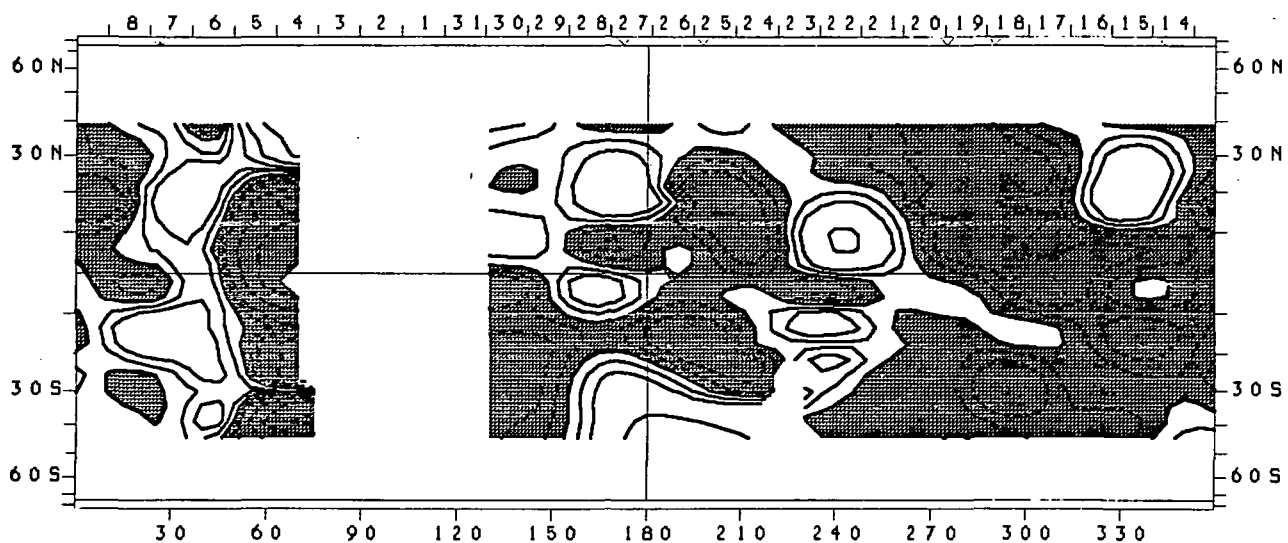
Figure 2: Synoptic maps of east-west velocity V_{west} for three consecutive rotations in 1979 (part a), in 1981 (part b), and in 1984 (part c). Westward moving regions are shown in unshaded. Eastward moving regions are shaded dark. The contour levels are $\pm 10, 20, 50, \dots$ m/s.

JUL 1979



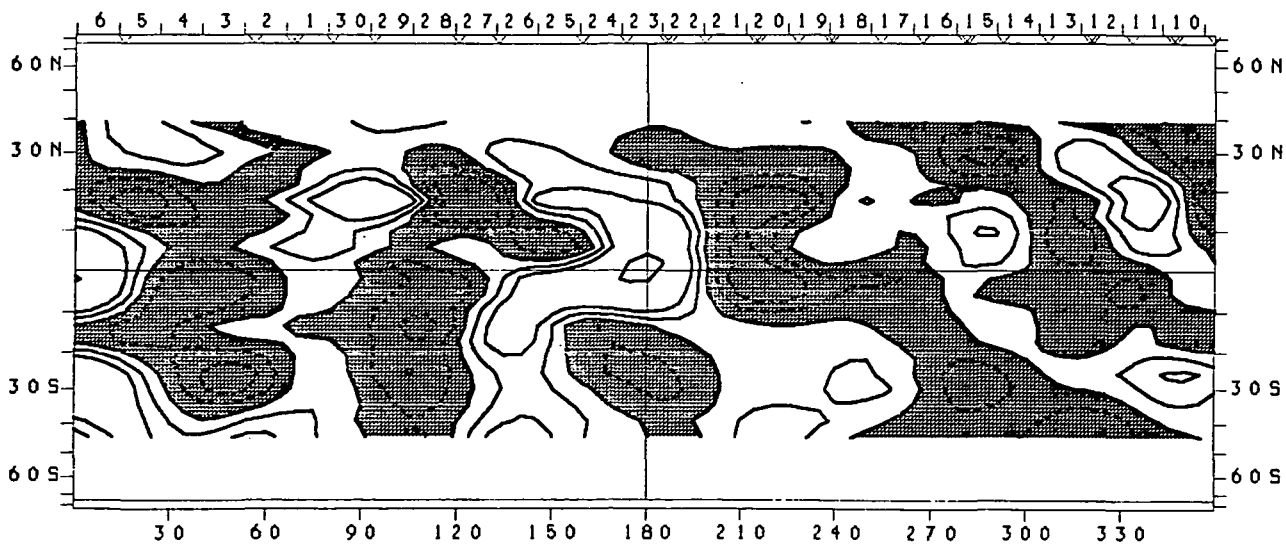
1684

AUG 1979



1685

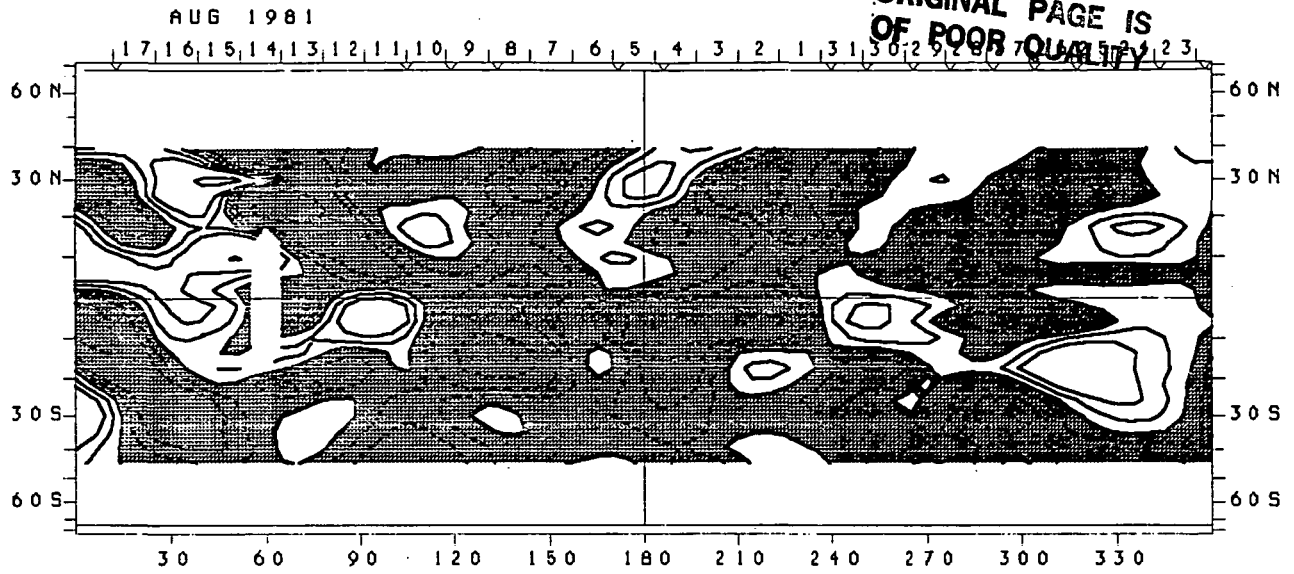
SEP 1979



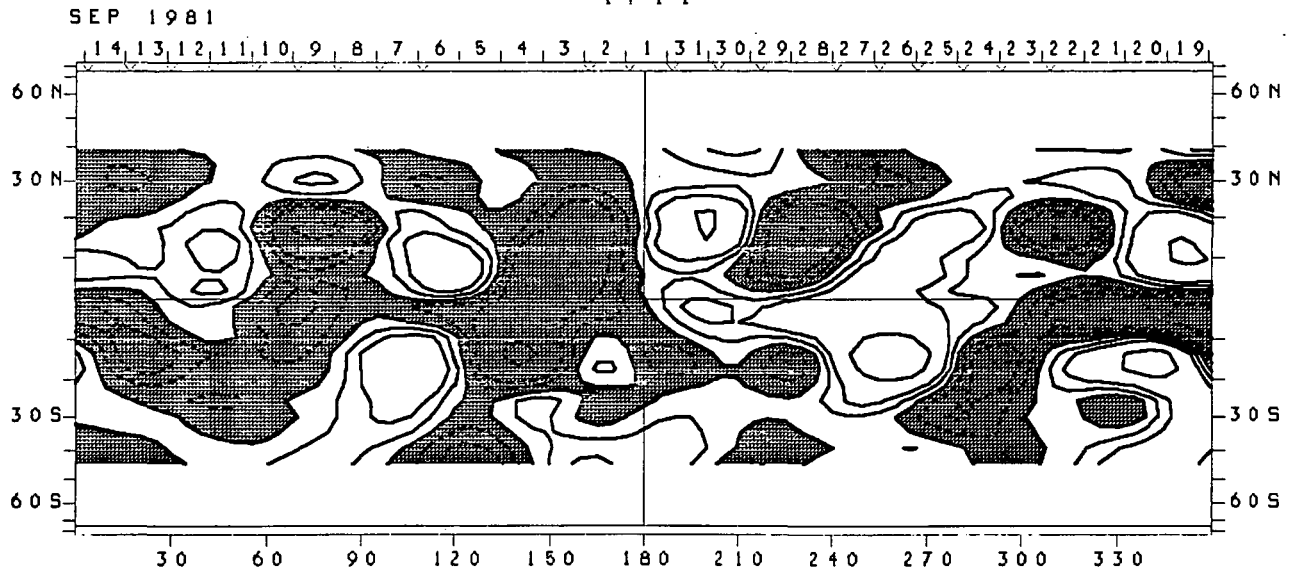
1686

Figure 2a

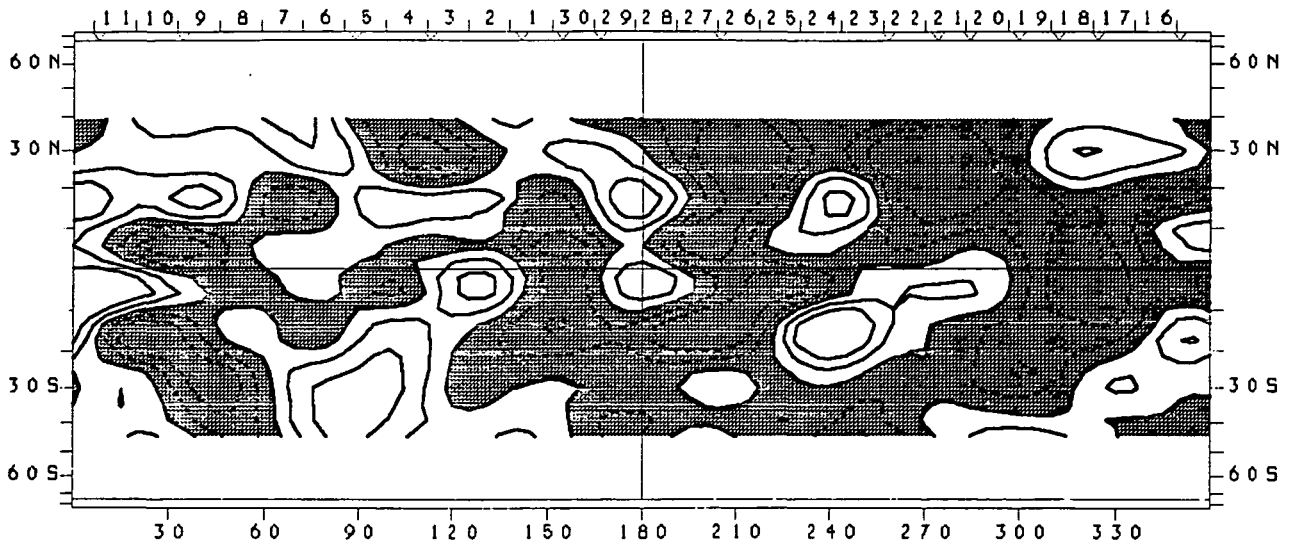
ORIGINAL PAGE IS
OF POOR QUALITY



17 11



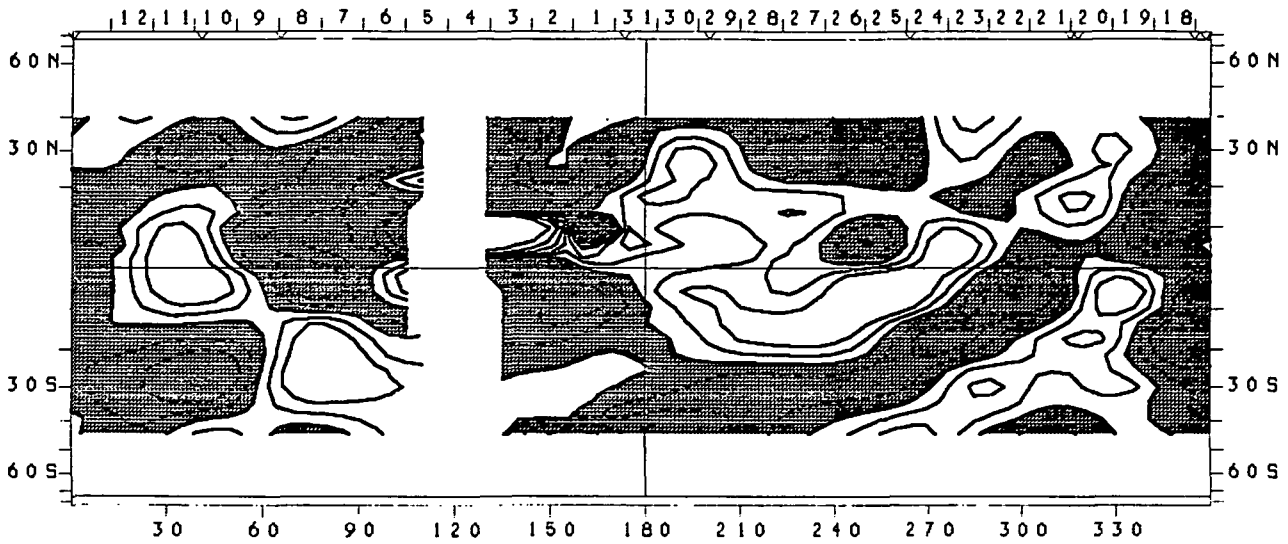
17 12
SEP 1981



17 13

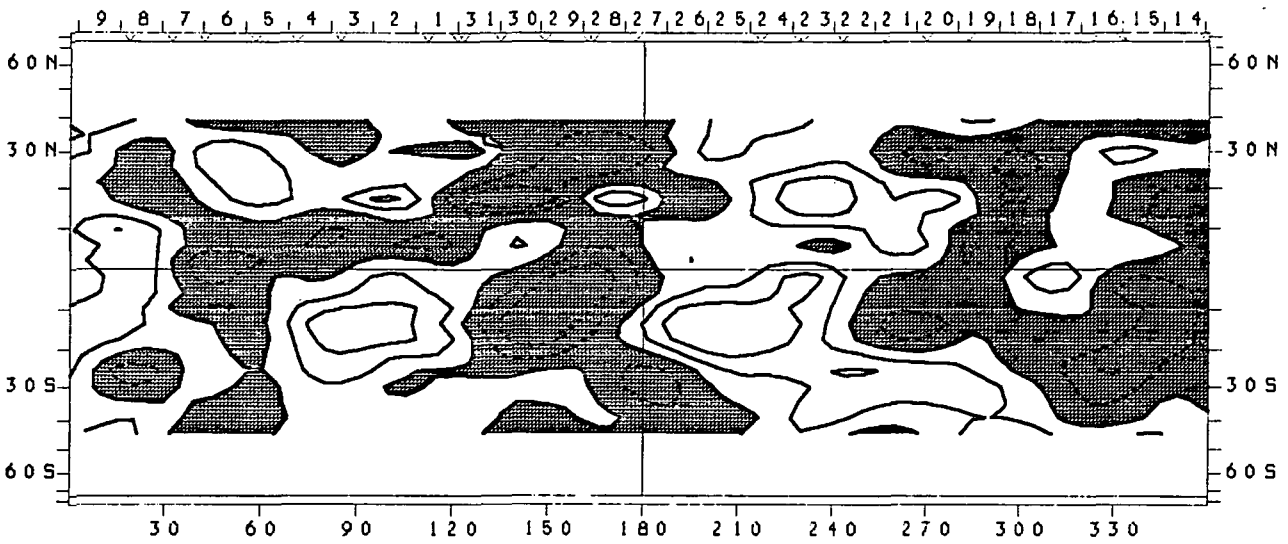
Figure 2b

JUL 1984



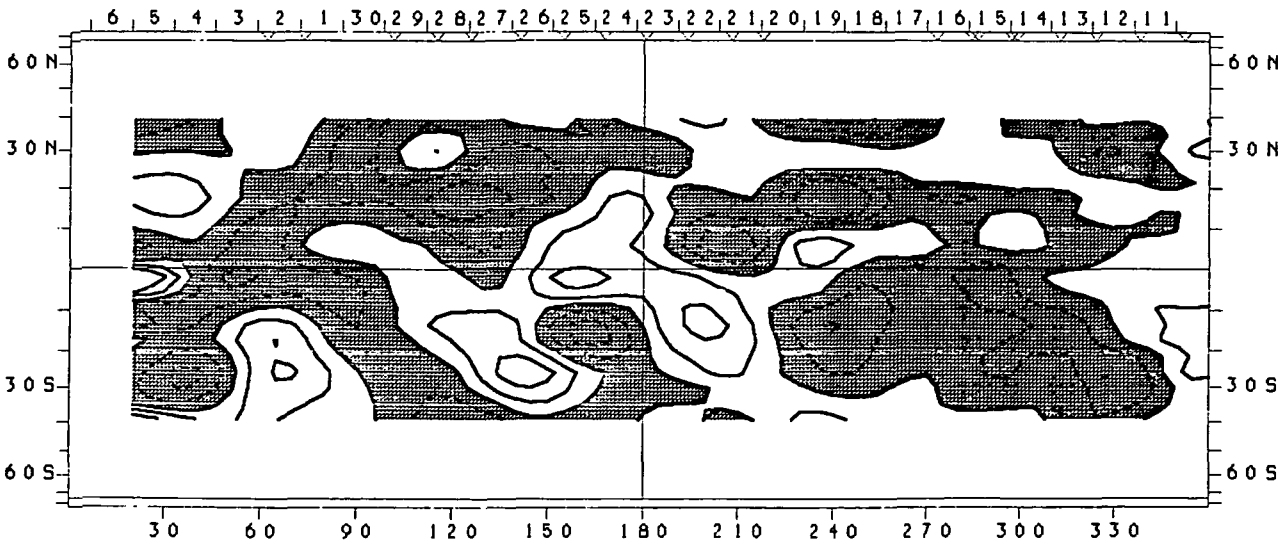
1751

AUG 1984



1752

SEP 1984



1753

Figure 2c

sequences than are presently available.

The intervals presented in Figure 2 were chosen both because of sufficient data coverage to show nearly complete maps and because an initial survey had identified these intervals as times of simple modal structure. This survey was done by computing power spectra of V_{west} for intervals of nearly continuous data coverage. It is interesting to note that the day-to-day variation in the whole-disc fit equatorial rotation rate (Scherrer et al., 1980) is very similar to the meridional average of V_{west} for the intervals examined. This was examined both by comparing power spectra and by inspection of the raw data. Essentially all of the day-to-day variation in the full disc fit of rotation comes from the velocity structures described here.

These velocity patterns have a large amplitude compared to the upper limits reported in previous analyses of observations from Mt. Wilson (Snodgrass and Howard, 1984). However, we note that the present analysis of Stanford observations finds horizontal flow patterns which are different in structure, and larger in scale than those searched for in the Mt. Wilson studies.

The complete understanding of the flow patterns reported here will require an extended set of high quality continuous observations throughout a solar cycle. The present results have been obtained with the instrument at Stanford. This instrument at present is limited to low resolution measurements and seldom has more than 30 or 40 days without interruption of a day or two. We are taking steps to increase both the resolution and the Doppler zero stability for future observations. We are also examining the comparable data of improved quality available from Mt. Wilson since 1982. We hope to be able to test our interpretation of the Stanford observations as signatures of the global convection and to begin the process of examining the morphology of these flows by comparisons with other data and further observations.

Acknowledgements: We thank Harald Henning for useful comments. This work was supported in part by the Office of Naval Research under Contract N00014-76-C-0207, by the National Aeronautics and Space Administration under Grant NGR5-020-559, and by the Atmospheric Sciences Section of the National Science Foundation under Grant ATM77-20580.

References

F. Cavallini, G. Ceppatelli, and A. Righini, Meridional and Equatorial Center to Limb Variation of the Asymmetry and Shift of three Fe I Solar Photospheric Lines Around 6300A, Astron. and Astrophys. in press(1985).

B. R. Durney, L. E. Cram, D. B. Guenther, S. L. Keil, and D. M. Lytle, A Search for Long-Lived Velocity Fields at the Solar Poles, Ap. J. 292(1985), 752-762.

Thomas L. Duvall, Jr., Large-Scale Solar Velocity Fields, Sol. Phys. 63(1979), 3-15.

Robert Howard and Hirokazu Yoshimura, Differential Rotation and Global-

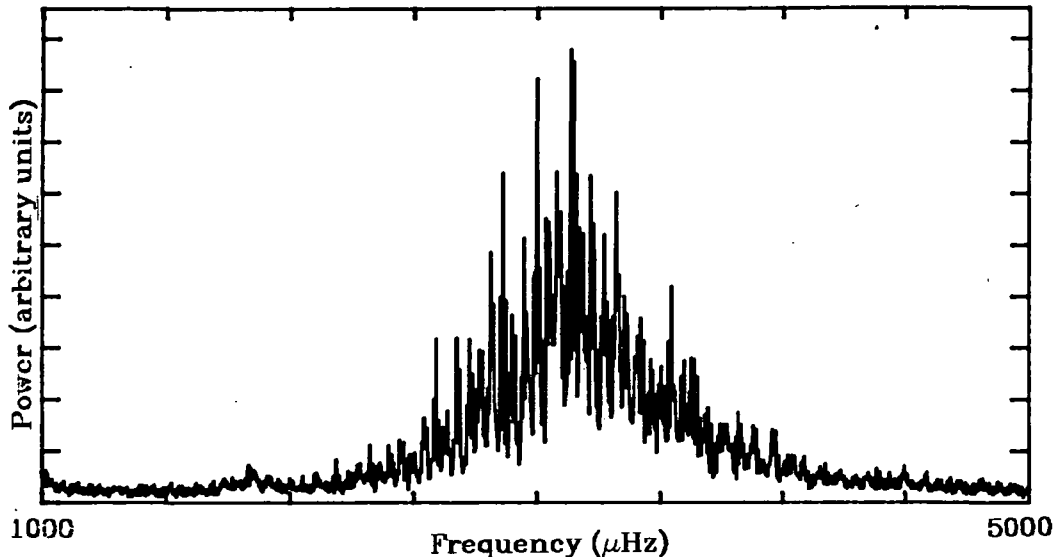


Figure 1

The power spectrum of the full data, from 1000 μHz to 5000 μHz .

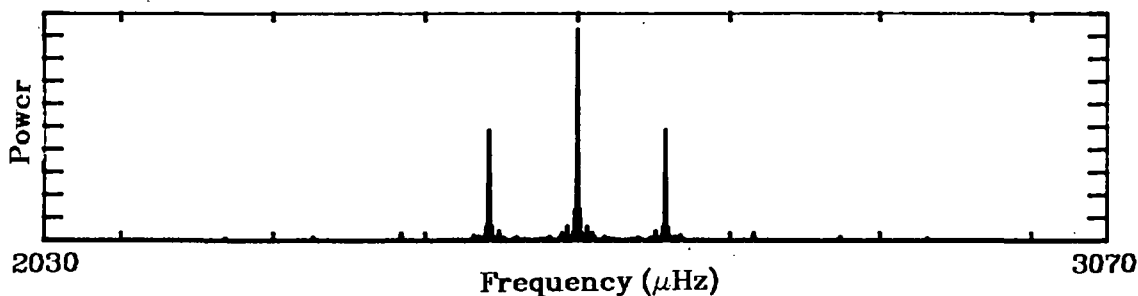


Figure 2

The window function: power spectrum of a 3000 μHz sine wave put into the actual data window.

to the main peaks greatly affect the fine scale structure of the spectrum and make the identification of individual peaks difficult.

In addition to the complications introduced by the window, the effects of splitting due to rotation and lifetimes, each producing multiple peaks with sidelobes, as well as noise make the spectrum very complex. Several computerized deconvolution and peak-subtracting techniques failed to make significant inroads on the problem (Scherrer 1985). A scheme combining computed power spectra and manual pattern recognition was decided upon as the best method to identify real solar peaks. Figures 3 and 4 are typical examples of the graphs used. These figures each show a section of the spectrum computed with several resolutions. Frequency runs along the abscissa, with each panel covering the same span, from 1432 μHz to 1572 μHz in figure 3, and from 3200 μHz to 3340 μHz in figure 4. We realized that the full resolution spectrum (panel E) is too complex to enable recognition of any given peak as a

ORIGINAL PAGE IS
OF POOR QUALITY

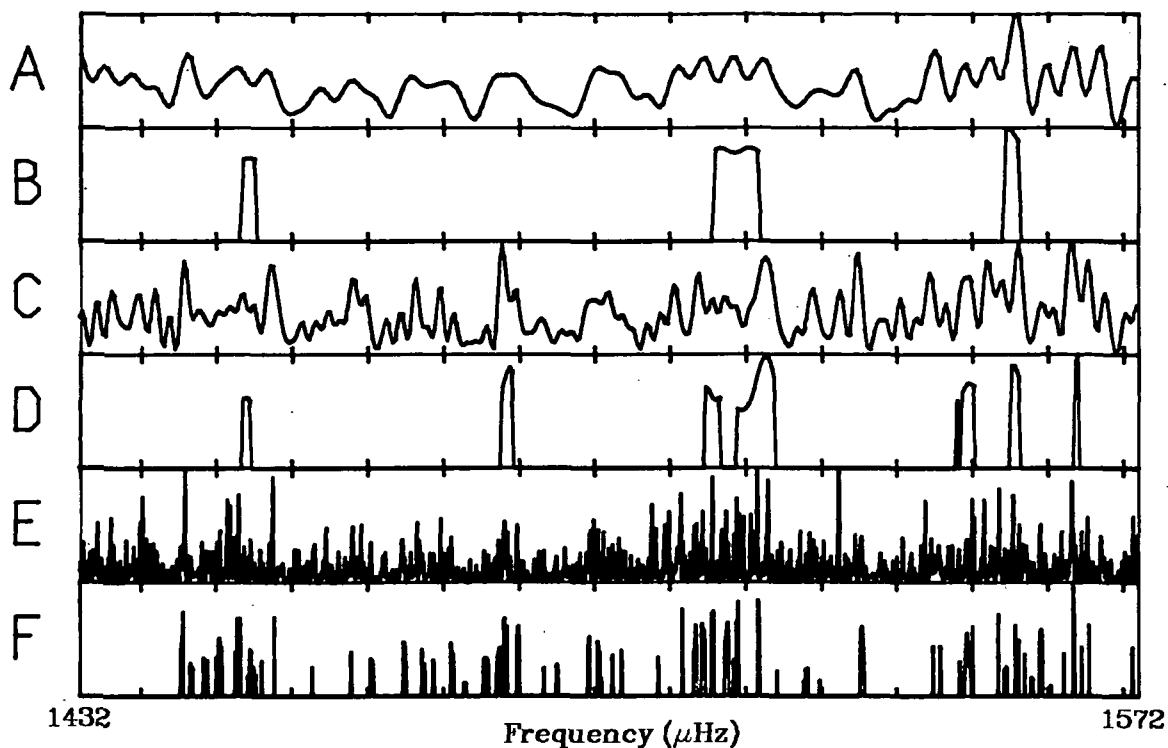


Figure 3

Plot of data in the frequency range from 1432 μHz to 1572 μHz :

A) average power spectrum of 4 day chunks of data, B) peak search on A,
C) average power spectrum of 8 day chunks of data, D) peak search on C,
E) full resolution power spectrum, F) peak search on E.

solar oscillation mode. At lower resolution, however, it becomes much clearer to see where there is power in the spectrum. Thus, the average of 6 spectra of 4-day segments of the data is plotted in panel A. Panel C shows the average of 3 spectra of 8-day segments of the data. To further aid in locating modes a simple computer program was used to scan the spectra, looking for structures which correspond to the main features of the window function, i.e. a central peak with two sidelobes at 1/day distance and of about 50% magnitude. The scan allowed the sidelobes to be as large as 90% or as small as 20% of the central peak. The program took the value of the spectrum at a frequency if it corresponded to a possible central peak and zero otherwise. The results of this search are plotted below the corresponding spectrum, in panels B, D and F. This composite graph proves to be a very useful tool in determining the frequencies of the modes. The first four panels, A-D, serve to locate and emphasize small frequency ranges where there is power. Using this information and a transparency with the window function plotted on it, one can then pinpoint the group of peaks (and its sidelobes) in the high-resolution full spectrum, panels E and F, that correspond to a solar p-mode. The frequency recorded for each mode was

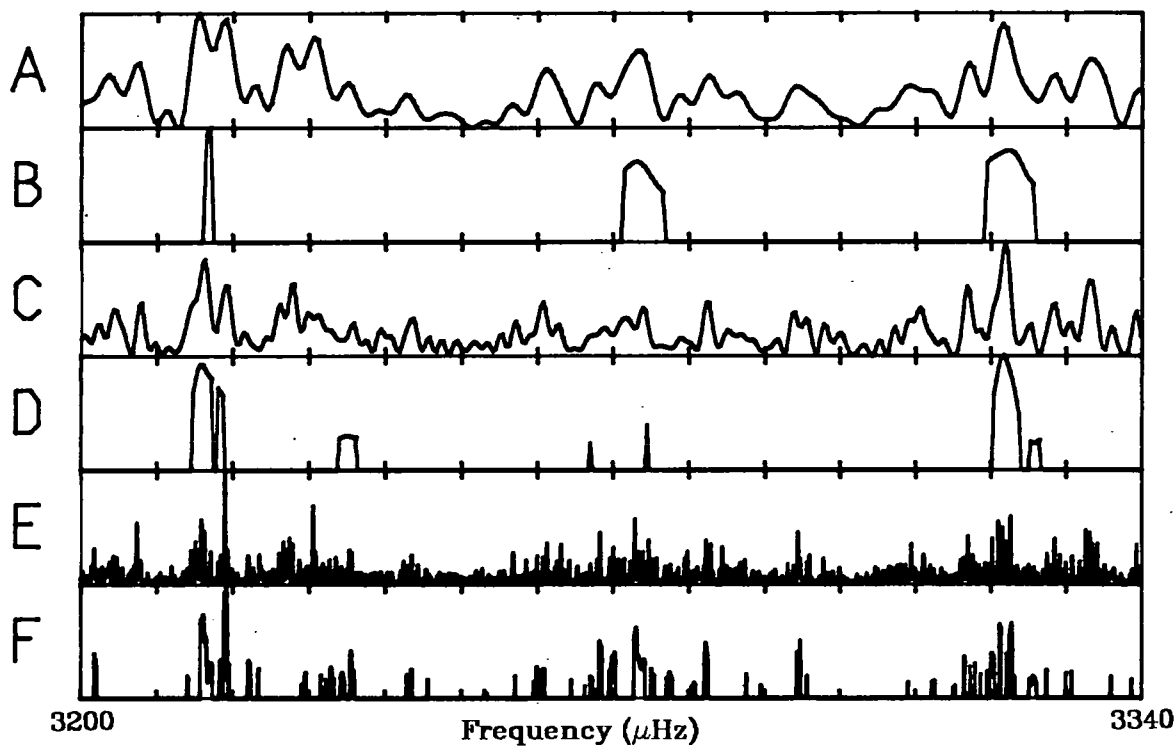


Figure 4
As figure 3, but for the range from 3200 μHz to 3340 μHz .

that of the central peak or approximate center of the group of peaks. A conservative estimate of the error in the frequency of any given mode is 2 μHz .

Analyzing the spectrum, we located modes ranging from 1035 μHz up to 5008 μHz . Identification of the modes was accomplished using previously published frequencies (Duvall and Harvey 1983, Duvall - private communication) for modes in the range from about 2000 to 4000 μHz as "anchors" for the determination of order n and degree l . The fact that the Stanford instrument is most sensitive to modes of degree 2 through 5 prevents confusion with higher degrees, although those modes certainly contribute to the "noise". Modes with frequencies outside of this range were then identified by making an echelle diagram (figure 5) and following the curve described by different n values of a given l . It is important to note that although there certainly is some bias in the location and identification of the modes with previously published frequencies, there is no such bias in the frequencies of modes of lower and higher order, since there was no preconception of where they should be. Table I lists the frequencies of the identified modes.

In addition to identification of the modes, we have also examined the data for evidence of rotational splitting. As mentioned before, the power of each mode is split into a multitude of peaks resulting from a combination of mode lifetimes, window function, and noise, as well as rotational splitting. This confusion effectively prevents one from

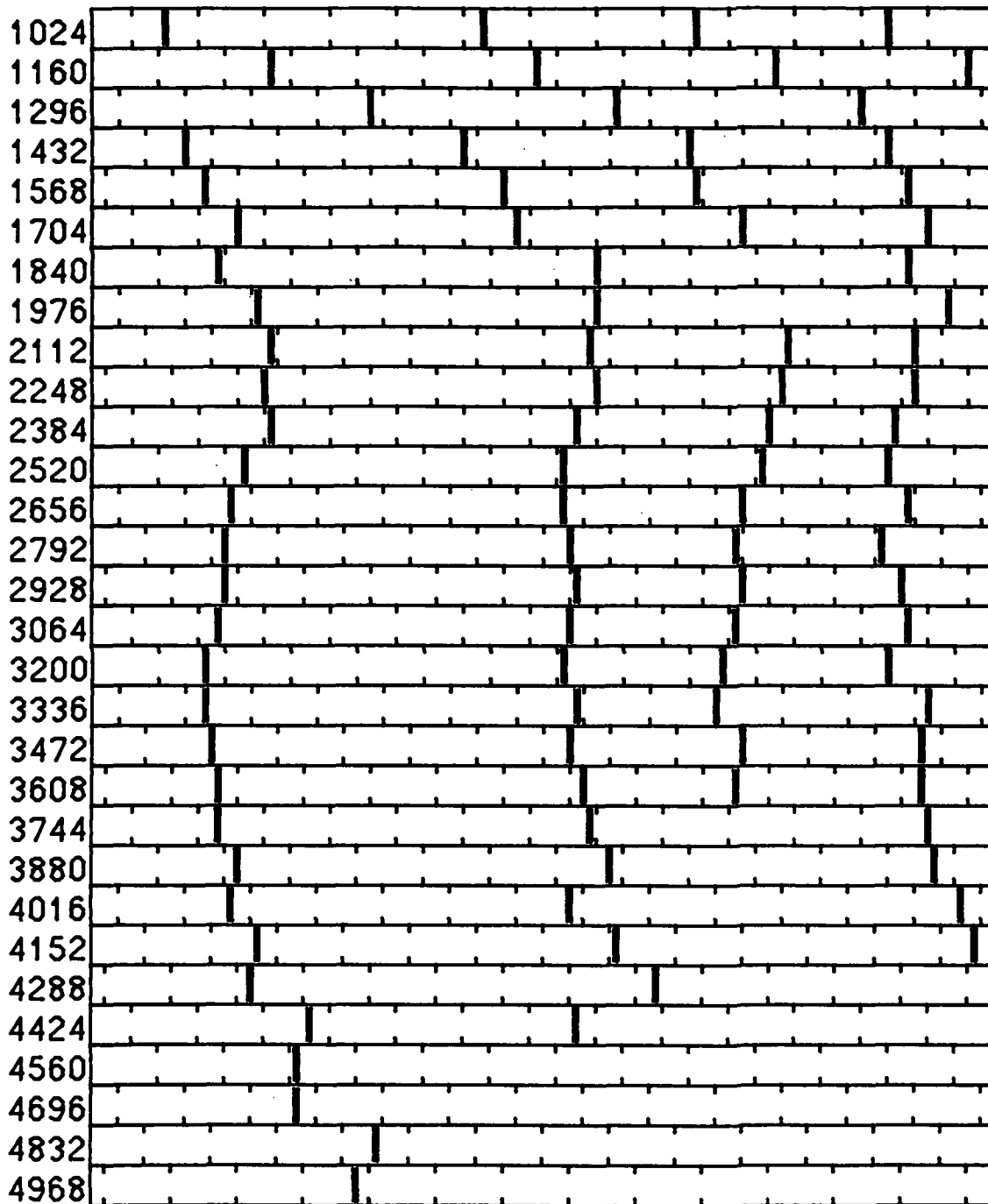


Figure 5
 Echelle diagram of the identified modes, each strip covers 136 μ Hz.

n	frequency				n	frequency			
	l=2	l=3	l=4	l=5		l=2	l=3	l=4	l=5
5			1035	1115	20	3026	3083	3136	3187
6	1083	1144	1187	1263	21	3161	3217	3271	3320
7	1227	1292	1338	1412	22	3295	3353	3409	3462
8	1375	1446	1488	1552	23	3430	3490	3544	3597
9	1522	1585	1630	1691	24	3570	3627	3682	3733
10	1659	1726	1768	1830	25	3705	3763	3819	3870
11	1802	1859	1916	1963	26		3902	3958	4007
12		2001	2052	2105	27		4037	4088	4147
13		2139	2187	2236	28		4177	4231	4285
14	2217	2274	2052	2372	29		4312	4373	
15	2352	2411	2457	2505	30		4457	4497	
16	2486	2543	2591	2640	31		4591		
17	2621	2677	2727	2779	32		4727		
18	2754	2812	2864	2911	33		4875		
19	2889	2948	3001	3050	34		5008		

Table I - Frequencies of identified modes

assigning m -values to given peaks and directly measuring the splitting. Rather, we have analyzed the spectrum using autocorrelations. Using the determined frequencies we calculated the autocorrelation of a small section of the full spectrum around each mode. All autocorrelations with a given degree l , but different order n , were then averaged together. The assumption is that any rotational splitting will not change much with order n . The results are plotted in the first four panels of figure 6. An autocorrelation of the window function is shown in the last panel of figure 6. It can be seen that the window is responsible for much of the systematic splitting, as evidenced by the peaks in its autocorrelation which are repeated and actually dominate the autocorrelations of the modes. However, all degrees show a peak around $0.8 \mu\text{Hz}$, which is close to twice the rotational splitting as measured by Duvall and Harvey (1984). Since the Stanford instrument is sensitive only to modes with $l+m$ even, this peak can be identified as the result of rotational splitting.

2. CONCLUSION

We have determined the frequencies of over 20 modes which have not been identified before. The majority of these modes lies in the frequency range from $1035 \mu\text{Hz}$ to $1800 \mu\text{Hz}$. The echelle diagram of the modes shows clearly the change in slope at low n , as the modes become spread further apart than $136 \mu\text{Hz}$. Also, we have been able to see a characteristic splitting which is consistent with the rotational splittings measured by

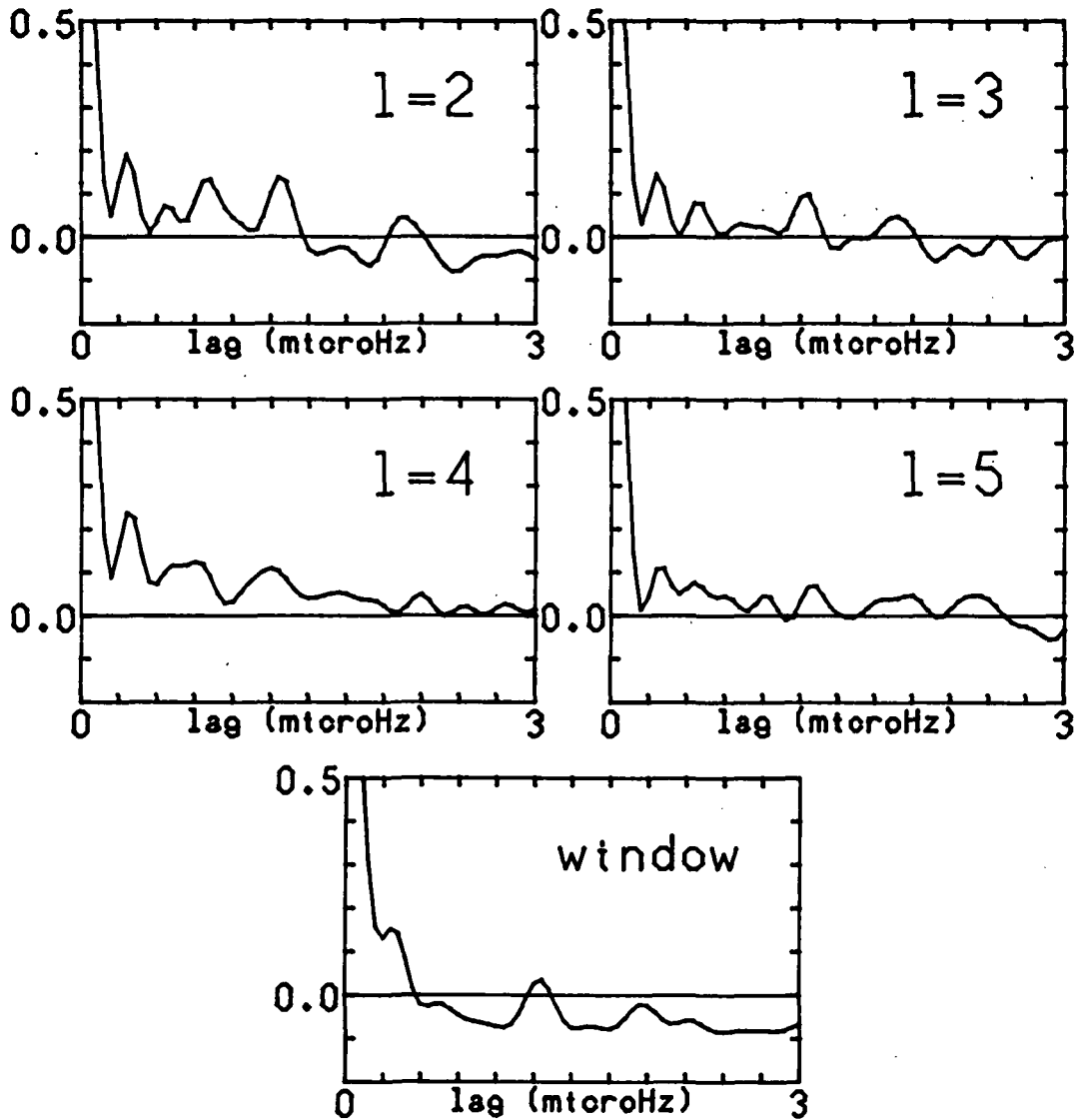


Figure 6

Autocorrelations of the power spectrum around different degrees l and the window function.

Duvall and Harvey (1984). Future examination of other Stanford data will hopefully refine the values, although no other year has had data as complete as 1984.

3. REFERENCES

Duvall Jr., T. L., and J. W. Harvey, 'Frequency spectrum of solar 5-minute oscillations with degree less than 140', *Nature*, 302, 24, 1983.

Duvall Jr., T. L., and J. W. Harvey, 'Rotational frequency splitting of solar oscillations', Nature, 310, 19, 1984.
Scherrer, P. H., J. M. Wilcox, J. Christensen-Dalsgaard, and D. O. Gough, 'Detection of solar five-minute oscillations of low degree', Solar Physics, 82, 75, 1983.
Scherrer, P. H., 'Comments on techniques for spectral deconvolution', these proceedings, 1985.

4. ACKNOWLEDGEMENTS

This work was supported in part by the Office of Naval Research under Contract N00014-76-C-0207, by the National Aeronautics and Space Administration under Grant NGR5-020-559, and by the Atmospheric Sciences Section of the National Science Foundation under Grant ATM77-20580.

N86-19278

COMMENTS ON TECHNIQUES FOR SPECTRAL DECONVOLUTION

Philip H. Scherrer,
Center for Space Science and Astrophysics
Stanford University
Stanford, California
U.S.A.

ABSTRACT. Current observational questions in asteroseismology require high spectral resolution that can only be obtained with observations spanning many days or months. The primary constraint in the full utilization of single mid-latitude observing sites is the presence of diurnal data gaps. Several methods for removing the effect of these gaps in the spectra obtained from velocity observations have been suggested. In the case of data coverage of less than 50%, none of the methods considered has been successful at unambiguously recovering the true spectrum from test spectra with realistic complexity. The limitations of these methods and their applicability to the helioseismology problem is discussed.

The presence of data gaps is particularly troublesome when computing power spectra of multi-day observations of solar or stellar oscillations. If the expected lifetime of the observed modes is longer than individual uninterrupted observing sequences, one naturally wants to combine many days of data to obtain higher spectral resolution. The gaps from nights or poor weather produce a complicated structure of sidebands in the power spectrum unless the gaps are filled with estimated data. Since the power spectrum is computed from the Fourier transform, and the observed transform can be considered as the convolution of the true spectrum and the transform of the observing window, filling the gaps is essentially a deconvolution process. Since there are an unlimited number of ways to fill the gaps with data, most of them non-physical, we must have some guidance from our a priori knowledge of the sun or star in question and we must have some method for incorporating this knowledge in an analytical procedure. Thus the whole problem of deconvolution or gap-filling is one of explicitly recognizing the assumptions about the star and finding objective ways to incorporate those assumptions in the analysis.

This problem is not unique to asteroseismology. In fact, there is a significant body of literature dealing with the deconvolution problem. The specific problems of asteroseismology are different from many of the previous applications however, so care must be exercised in applying previously developed methods. Some of the particular problems of solar

and stellar observations are low filling factors (i.e. large gaps relative to intervals of continuous data), very complex spectra with thousands of modes allowed over several decades in frequency, line separation on the same order as the main contributions from typical observing windows, and low signal to noise in frequency bands that contain important oscillation modes. A number of gap-filling methods have been suggested for the asteroseismology problem. These include maximum entropy methods of "predicting" the data in the gaps (Fahlman and Ulrych, 1982), variations of the CLEAN algorithm of iterative peak subtraction (Scherrer, 1984), rearranging the data to fill the gaps at the expense of resolution (Kuhn, 1982), and iterative multiplicative deconvolution (Connes and Connes, 1984).

Brown and Christensen-Dalsgaard (1985) have completed a thorough study of the applicability of the maximum entropy method to the problem. They found that complex spectra can be correctly recovered provided the filling factor is high (greater than 0.8) and the signal-to-noise ratio is high (greater than 100). Fortunately, these conditions are expected to be met for p-mode observations from an earth-bound network. They found that as the filling factor dropped below 0.5 or the s/n dropped below about 30 the error rate increased rapidly. Kuhn found similar results when applying the data-swapping method to data with a low filling factor (Kuhn et al., 1985).

Delache and Scherrer (1983) successfully applied the CLEAN-like iterative peak subtraction method to low-filling factor observations in the long-period spectral region but that method was not successful when applied to p-mode spectra (Henning and Scherrer, 1985). Experiments with linear iterative deconvolution methods have not been as successful as the CLEAN technique. There is a tendency for noise peaks to grow rather than to be simply extracted unchanged as in the CLEAN method. This is a characteristic of linear iterative methods (Jansson, 1984).

In order to push these procedures to the regime of low-filling factor, the methodology of inserting a priori knowledge into the analysis must be explicitly examined. There are different assumptions implicitly made by the various methods. The maximum entropy method assumes that the signal is locally stationary. This is a fairly weak assumption and leads to failure when the gaps are large. The stronger assumption of completely stationary signals made in the CLEAN method can do a better job of recovering the true spectrum with low filling factors, but only in cases where the assumption is valid. Thus, the long period success and the p-mode failure of the method.

Particularly strong claims have been made for the advantages of the non-linear spectral deconvolution method (Connes and Connes, 1984). This has led to a careful examination of the applicability of that method to the problem. The method can be summarized as the iterative task of finding a spectrum that when convolved with the window function yields the observed spectrum. The iteration is done under some constraints that provide the mechanism for including prior knowledge. This method has the advantage of explicitly specifying the assumptions. It has been applied for some time to the deconvolution of instrumental profiles from spectra and has been described by (Blass and Halsey, 1981) for that application. The general method has been examined by a number

of authors in other applications and it has been shown that convergence can be guaranteed in many cases (Sanz and Huang, 1983, Schafer et al., 1981). A general discussions of both subtractive and multiplicative deconvolution techniques have been presented by Bates and colleagues (Bates et al., 1982a, 1982b, 1982c) and by Jansson (1984).

Connes and Connes suggested applying the multiplicative deconvolution method independently to the real and imaginary parts of the Fourier transform of oscillation observations. It turns out that constraints suggested do not quite match the problem. In particular, the method assumes that the true signal is band-limited, and that power outside the known band comes from the gaps. Unfortunately, it is not possible to arrange the observations of the sun (or many stars) to match this criterion. The p-mode frequency band, for example, extends from possibly 300 micro-Hz through 4500 micro-Hz. The sidebands from nightly gaps are spaced at about 11.6 micro-Hz. Thus most of the sidebands are within the desired frequency band. The method probably works but is expected to be rather inefficient. Thus, this method at present does not solve our problem (J. Connes, private communication, 1985).

What has yet to be done, is to find a methodology for tuning an analysis to specific prior knowledge or assumptions. For example, if we were asking what is the rotational splitting for solar p-modes, then since we know the central frequencies for each multiplet (to a few micro-Hz) we should be able to tell our analysis procedure just where power is from gaps and where it is probably of solar origin. If we believe that the lifetime of low-frequency p-modes is several months but the lifetime of high-frequency modes may be only a few days, we should be able to find peak centroids using varying resolution across the p-mode band. Perhaps the iterative methods can be adapted to such more problem-specific constraints. In any case, we must always be aware of the explicit and implicit assumptions in our procedures. In summary, two things are clear: First, if we do not attempt to account for the sidebands introduced by the data gaps we are making the implicit assumption that the sun does not oscillate at night and second, we do not yet have a reliable, objective method for filling the gaps in the case of low filling factor.

Acknowledgements: This work was supported in part by the Office of Naval Research under Contract N00014-76-C-0207, by the National Aeronautics and Space Administration under Grant NGR5-020-559, and by the Atmospheric Sciences Section of the National Science Foundation under Grant ATM77-20580.

References

- J.H.T. Bates, W.R. Fright, R.P. Millane, A.D. Seagar, G.T.H. Bates, W.A. Norton, A.E. McKinnon, and R.H.T. Bates, Subtractive Image restoration. III. Some practical Applications, Optik 62(1982), 333-346.
- J.H.T. Bates, A.E. McKinnon, and R.H.T. Bates, Subtractive Image Restoration. II): Comparison with Multiplicative Deconvolution, Optik 62(1982), 1-14.

J.H.T. Bates, A.E. McKinnon, and R.H.T. Bates, Subtractive Image Restoration. I: Basic Theory, Optik 61(1982), 349-364.

William E. Blass and George W. Halsey, Deconvolution of Absorption Spectra, Academic Press, Inc., 1981.

Timothy M. Brown and Jorgen Christensen-Dalsgaard, A Technique for Filling Gaps in Time Series with Complicated Power Spectra, preprint, High Altitude Observatory, NCAR, 1985.

Janine Connes and Pierre Connes, A Numerical Solution of the Data-Gaps Problem, Space Research Prospects in Stellar Activity and Variability, Meudon Observatory, February 1984.

Philippe Delache and Philip H. Scherrer, Detection of Solar Gravity Mode Oscillations, Nature 306(December 15, 1983), 651-653.

G.G. Fahlman and T.J. Ulrych, A New Method for Estimating the Power Spectrum of Gapped Data, Mon. Not. R. astr. Soc. 199(1982), 53-65.

Harald M. Henning and Philip H. Scherrer, Observations of Low-Degree P-Mode Oscillations in 1984, These Proceedings, 1985.

Peter A. Jansson, ed., Deconvolution with Applications in Spectroscopy, Academic Press, Inc., 1984.

J.R. Kuhn, Recovering Spectral Information from Unevenly Sampled Data: Two Machine-Efficient Solutions, The Astronomical Journal 87,1 (January 1982), 196-202.

J.R. Kuhn, K.G. Libbrecht, and R.H. Dicke, Solar Ellipticity Fluctuations Yield No Evidence of g-Modes, submitted to Nature, 1985.

Jorge L.C. Sanz and Thomas S. Huang, Iterative Time-Limited Signal Restoration, IEEE Transactions on Acoustics, Speech, and Signal Processing ASSP-31,3 (June 1983), 643-650.

Ronald W. Schafer, Russell M. Mersereau, and Mark A. Richards, Constrained Iterative Restoration Algorithms, Proceedings of the IEEE 69,4 (April 1981), 432-450.

Philip H. Scherrer, Detection of Solar Gravity Mode Oscillations, in Solar Seismology From Space, A Conference at Snowmass, Colorado, R. K. Ulrich, J. Harvey, E. J. Rhodes, Jr., and J. Toomre (editor), NASA, December 15, 1984, 173-182.